2004A0609-NSa-np-Na BL27SU

Installation of SPELEEM to BL27SU and Application to Nanomaterial Studies

T.Koshikawa[a]*(14330), F.-Z.Guo[b](8451), T.Wakita[b](454), H.Shimizu[a](13889), A.Nakaguchi[a](14351), T.Yasue[a](14308), K.Ono[c](4037), T.Taniuchi[d](13620), Y.Watanabe[e](3410), H.Hibino[e](14324), T.Suzuki[e](6096), H.Daimon[f](1258), F.Matsui[f](5945), Y.Kato[f](13252), T.Kinoshita[g](14342), T.Okuda[g](14345), H.-L.Sun[g](14347), E.Bauer[h](14331), K.Kobayashi[b](1835)

[a]Osaka Electro-Commun. Univ., [b]JASRI, [c]KEK, [d]Univ. Tokyo, [e]NTT, [f]Nara Inst. Sci. Technol., [g]Inst. Solid State Phys, Univ. Tokyo, [h]Arizona State Univ.

Spectroscopic Photoemission and Low Energy Electron Microscope (SPELEEM) was installed to BL27SU, and its fundamental performance was examined. The samples observed were Co-patterned substrate, NiO, Iron oxide, In/Si(111) and Co-silicide/Si(111).

Fig. 1 shows a picture of the newly installed SPELEEM to BL 27SU. SR light comes from left side and irradiates the sample with the incident angle of 16° from the surface. Emitted electrons are accelerated to 20 keV between the sample and the objective lens, and go through imaging lenses and a hemispherical energy analyzer. Finally the image projected onto the screen.

Inset of fig. 2 shows the PEEM image of In/Si(111), whose field-of-view is 50 μm. The photon energy was 500 eV, and emitted secondary electrons are imaged. The 3D In crystal is seen in the middle of the image, and the rest is 2D In layer which consists of two atomic layers. Selected-area In $3d_{5/2}$ XPS spectra taken at circles are indicated in fig. 2. (a) is the XPS spectrum for 3D crystal and (b) that for 2D layer. The spectral width in (b) is broader than that in (a) and a faint shoulder can be recognized in (b) at low binding energy side. Solid lines show the results of curve fitting using Gaussian. For 3D crystal, there is only one component, while two components for 2D layer as shown by broken lines. The chemical shifts relative to the peak for 3D crystal are -0.18 eV and 0.14 eV, respectively. It is considered that these chemical shifts are due to Si-In and In-In bonding in 2D layer.

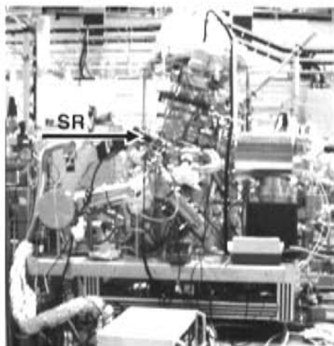

Fig. 1. Picture of SPELEEM installed to BL27SU.

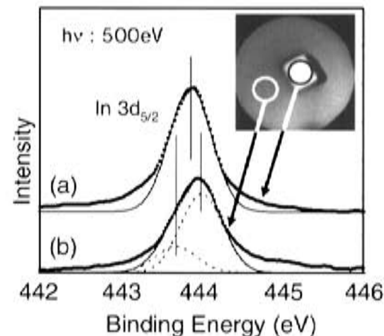

Fig. 2. Selected-area In $3d_{5/2}$ XPS spectra from (a) 3D In island and (b) 2D layer of In/Si(111).

2004A0034-ND3c-np BL28B2

Characterization of dislocations in orthorhombic lysozyme crystals by using synchrotron white beam topography

Miki Shimizu 9262[1], Haruhiko Koizumi 7007[1], Takashi Uchida 7217[1], Natsuko Aota 8624[1], Masaru Tachibana 5742*[1], Kunihide Izumi 1824[2], Kentarou Kajiwara 1794[2]

[1]Graduate School of Integrated Science, Yokohama City University, Yokohama 236-0027
[2]Spring-8/JASRI, Mikazuki Hyogo 679-5198

The characterization of defects in protein crystals is very important for an understanding of their crystallization. X-ray topography using synchrotron radiation is one of the most powerful methods to characterize crystal defects because a large number of topographs with different reflections can be obtained by one short exposure. We have succeeded in observation of X-ray topographs of tetragonal lysozyme crystals [1]. In this paper, we first report the determination of indexes of topographs and the characterization of the dislocations in orthorhombic lysozyme crystals using synchrotron white beam topography.

Fig. 1 shows X-ray topographs of an orthorhombic lysozyme crystal taken by using synchrotron white beam. However, each Laue topograph includes higher-order crystallographic reflections with harmonic wavelengths. The relative diffracted intensities I_h contributed by the harmonic components were calculated using the equation [2]:

$$I_h = P(\lambda) F_{hkl} \lambda^3 \mathrm{cosec}^2 \theta \exp(-\mu t),$$

where $P(\lambda)$ is the distribution of X-ray intensity with wavelength λ arriving at the specimen, F_{hkl} is the structure factor for the reflection, θ is the Bragg angle, μ is the linear absorption coefficient and t is the thickness of the crystal. Here, the absorption has been described roughly by the factor $\exp(-\mu t)$. Table 1 shows the calculated relative intensities I_h corresponding to harmonic reflections, 111, 222, 333 and so on, included in the topograph of Fig. 1(a) and (b). According to Table 1, the predominant component contributed to Fig. 1(a) is found to be 111 crystallographic reflection. Similarly, the predominant component contributed to Fig. 1(b) is found to be 450 reflection.

As shown in Fig. 1, clear straight lines from the core part of the orthorhombic lysozyme crystal are growth-in dislocations, since these lines are similar to those of the dislocations commonly observed in solution-growth crystals [3]. According to dislocation invisibility in Fig. 1, it is found that predominant growth-in dislocations are of edge character with <001> Burgers vector.

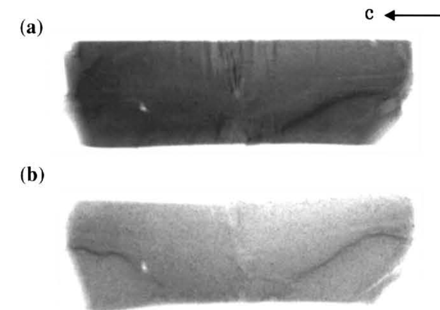

Fig.1 Laue topographs in (a) 111, (b) 450 reflections, respectively.

	reflection	θ(deg)	λ(Å)	$\lvert F_{hkl}\rvert$	$P(\lambda)$	$\exp(-\mu t)$	I_h
a	**[1 1 1]**	1.37	1.207	78.83	1.48	0.479	**530.9**
	[2 2 2]	1.37	0.6036	75.87	3.08	3.64	55.09
	[3 3 3]	1.37	0.4024	58.73	5.97	11.9	1.7
	[4 4 4]	1.37	0.3018	12.48	37.5	27.6	0.02
b	**[4 5 0]**	2.12	0.7528	88.93	2.11	1.91	**93.95**
	[8 10 0]	2.12	0.3764	21.78	17.2	14.5	0.14

Table.1 Relative intensities I_h corresponding to harmonic reflections.

Reference

[1] M. Tachibana *et al.*, *J.Synchrotron Rad.*, **10** (2003) 416
[2] T. Tuomi *et al.*, *Phys. Stat. Sol. (a)*, **25** (1974) 93.
[3] K. Kojima, *Progress Crystal Growth and Characteristics of Materials* (Pergamon Press, London, 1992) 369.